A Posteriori Error Estimator Competition for Conforming Obstacle Problems

C. Carstensen,[1,2] **C. Merdon**[1,2]
[1] *Humboldt-Universität zu Berlin, Unter den Linden 6, 10099 Berlin, Germany*

[2] *Department of Computational Science and Engineering, Yonsei University, 120-749 Seoul, Korea*

Received 25 March 2011; accepted 12 March 2012
Published online in Wiley Online Library (wileyonlinelibrary.com).
DOI 10.1002/num.21728

This article on the a posteriori error analysis of the obstacle problem with affine obstacles and Courant finite elements compares five classes of error estimates for accurate guaranteed error control. To treat interesting computational benchmarks, the first part extends the Braess methodology from 2005 of the resulting a posteriori error control to mixed inhomogeneous boundary conditions. The resulting guaranteed global upper bound involves some auxiliary partial differential equation and leads to four contributions with explicit constants. Their efficiency is examined affirmatively for five benchmark examples. © 2012 Wiley Periodicals, Inc. Numer Methods Partial Differential Eq 00: 000–000, 2012

Keywords: adaptive finite element methods; a posteriori error estimators; elliptic variational inequalities; obstacle problems

I. INTRODUCTION

The a posteriori error analysis is well developed for variational problems of second-order elliptic partial differential equations with explicit constants and at least five different types of error estimators. Considerably less is known about the a posteriori error control for variational inequalities, in particular, for its model obstacle problem [1–8]. Braess' error estimator split for an obstacle problem [6] leads to some computable term with an extended discrete Lagrange multiplier plus the Galerkin discretization error of an auxiliary variational equation.

Given a bounded Lipschitz domain $\Omega \subset \mathbb{R}^2$ with boundary $\partial\Omega$ and its closed subset Γ_D of positive surface measure, the data of the obstacle problem are the right-hand sides $f \in H^1(\Omega)$ and $g \in L^2(\Gamma_N)$ on $\Gamma_N := \partial\Omega \backslash \Gamma_D$ plus the Dirichlet data $u_D \in C^0(\Gamma_D)$ edgewise in H^2 and the

Correspondence to: C. Carstensen, Humboldt-Universität zu Berlin, Unter den Linden 6, 10099 Berlin, Germany (e-mail: cc@mathematik.hu-berlin.de)
Contract grant sponsor: Ministry of Education, Science and Technology (National Research Foundation of Korea, NRF [by DFG Research Center MATHEON and World Class University, WCU]); contract grant number: R31-2008-000-10049-0

obstacle χ in $H^1(\Omega) \cap C^0(\overline{\Omega})$ with $\chi \leq u_D$ along Γ_D. The weak form relies on the closed and convex set

$$K := \{v \in H^1(\Omega) | v = u_D \text{ on } \Gamma_D \text{ and } \chi \leq v \text{ a.e. in } \Omega\} \neq \varnothing.$$

The obstacle problem reads: Seek $u \in K$ such that

$$a(u, u - v) \leq F(u - v) \text{ for all } v \in K. \tag{1.1}$$

Here and throughout the paper, we use standard notation for Lebesgue and Sobolev spaces and denote the energy norm

$$|||\cdot||| := a(\cdot, \cdot)^{1/2}$$

with respect to the bilinear form a in $H^1(\Omega)$,

$$a(u, v) := \int_\Omega \nabla u \cdot \nabla v \, dx \tag{1.2}$$

for all $u \in u_D + V$ and $v \in V := \{v \in H^1(\Omega) | v|_{\Gamma_D} = 0\}$. The right-hand side F in the dual $V^\star$ of V reads

$$F(v) := \int_\Omega f v \, dx + \int_{\Gamma_N} g v \, \mathrm{ds} \quad \text{for all } v \in V. \tag{1.3}$$

It is well known that (1.1) has a unique solution [9–11].

Given a regular triangulation $\mathcal{T}$ of Ω in the sense of Ciarlet [12, 13] with nodes $\mathcal{N}$ and nodal basis $(\varphi_z | z \in \mathcal{N})$ of the first-order finite element method, the nodal interpolation of $v \in C^0(\overline{\Omega})$ reads

$$\mathcal{I}v = \sum_{z \in \mathcal{N}} v(z) \varphi_z \in P_1(\mathcal{T}) \cap C^0(\overline{\Omega}).$$

The discrete version of problem (1.1) uses the discrete set

$$K(\mathcal{T}) := \{v_h \in P_1(\mathcal{T}) \cap C^0(\overline{\Omega}) | v_h = \mathcal{I}u_D \text{ on } \Gamma_D \text{ and } \mathcal{I}\chi \leq v_h \text{ in } \Omega\}$$

(with the piecewise affine functions $P_1(\mathcal{T})$) and reads: Seek $u_h \in K(\mathcal{T})$ such that

$$a(u_h, u_h - v_h) \leq F(u_h - v_h) \text{ for all } v_h \in K(\mathcal{T}). \tag{1.4}$$

The finite element method is called *conforming* if $K(\mathcal{T}) \subset K$, for instance, when $\chi = \mathcal{I}\chi$ equals its nodal interpolation $\mathcal{I}\chi$, and is called *nonconforming* otherwise.

After [6] and for a particular choice of Λ_h, the discrete solution of the obstacle problem u_h solves the discrete version of the Poisson problem for $w \in \mathcal{I}u_D + V$ with

$$a(w, v) = F(v) - \int_\Omega \Lambda_h v \, dx \quad \text{for all } v \in V. \tag{1.5}$$

The energy norm difference $|||w - u_h|||$ between u_h and the exact solution w of the Poisson problem (1.5) can be estimated by a large collection of error estimators [14–22], in particular the ones compared in [23, 24].

This article extends the result in [6] to problems with inhomogeneous Dirichlet boundary data. Suppose $w_D \in H^1(\Omega)$ satisfies $w_D|_{\Gamma_D} = u_D - \mathcal{I}u_D$ and $\chi - u_h \le w_D$. In the conforming case $\chi \le \mathcal{I}\chi$, our main result (Theorem 3.2) on w from (1.5) implies some computable global upper bound (GUB) slightly sharper than

$$|||e||| \le |||w - u_h||| + |||\Lambda_h - J\Lambda_h|||_* + \left(\int_\Omega (\chi - u_h - w_D) J\Lambda_h \, dx\right)^{1/2} + 2|||w_D|||. \tag{1.6}$$

This bounds the error $e := u - u_h$ in the energy norm by the error $|||w - u_h|||$. The first extra term

$$|||\Lambda_h - J\Lambda_h|||_* := \sup_{v \in V\setminus\{0\}} \int_\Omega (\Lambda_h - J\Lambda_h) v \, dx / |||v|||$$

relates to a nonpositive approximation $J\Lambda_h$ of Λ_h, while $\int_\Omega (\chi - u_h - w_D) J\Lambda_h \, dx$ contributes only on the transition between the contact zone and the noncontact zone. The term w_D refers to inhomogeneous Dirichlet data approximation and its minimal $H^1(\Omega)$ extension.

For affine obstacles, Theorem 4.1 proves efficiency in the sense of

$$\text{GUB} \lesssim |||e||| + |||\Lambda - \Lambda_h|||_*$$

up to pertubations that are of higher order, at least for benchmarks with $\Gamma_N := \varnothing$. The Lagrange multiplier Λ is defined below in (3.10).

The remaining parts of this article are organized as follows. The interpolation operator J and a suitable choice for w_D are described in Section II. Section III presents the details of our construction of Λ_h and discusses reliability of the above estimate. Section IV discusses its efficiency in case of affine obstacles. Section V describes an adaptive mesh refinement algorithm and six known a posteriori error estimators from Poisson problems for the estimation of $|||w - u_h|||$ in the GUB. Section VI discusses five computational benchmark examples. Two affine problems verify the theoretical findings and suggest that the overhead apart from the estimator contributions is *not* dominant.

II. PRELIMINARIES

Consider a regular triangulation $\mathcal{T}$ of $\Omega \subseteq \mathbb{R}^2$ with nodes $\mathcal{N}$, free nodes $\mathcal{M} := \mathcal{N}\setminus\Gamma_D$, fixed nodes $\mathcal{N}(\Gamma_D) := \mathcal{N}\setminus\mathcal{M}$, edges $\mathcal{E}$, Dirichlet edges $\mathcal{E}(\Gamma_D) := \{E \in \mathcal{E} | E \subseteq \Gamma_D\}$, Neumann edges $\mathcal{E}(\Gamma_N) := \{E \in \mathcal{E} | E \subseteq \overline{\Gamma}_N\}$, and interior edges $\mathcal{E}(\Omega) := \mathcal{E}\setminus(\mathcal{E}(\Gamma_D) \cup \mathcal{E}(\Gamma_N))$. Each node z in $\mathcal{N}$ is associated with its nodal basis functions φ_z and node patch $\omega_z := \{\varphi_z > 0\}$ with diameter $h_z := \operatorname{diam}(\omega_z)$. The quantity $h_\mathcal{E} \in P_0(\mathcal{E})$ denotes the local edge length, i.e., $h_\mathcal{E}|_E := h_E := |E|$ for $E \in \mathcal{E}$. Similarly, $h_\mathcal{T}$ denotes the local triangle diameter, $h_\mathcal{T}|_T := h_T := \operatorname{diam}(T)$ for $T \in \mathcal{T}$. Each element $T \in \mathcal{T}$ is the convex hull of the set $\mathcal{N}(T)$ of its three vertices and associated to its element patch $\omega_T := \bigcup_{z \in \mathcal{N}(T)} \omega_z$. The set $\mathcal{E}(T)$ denotes the edges on the boundary of T. For two expressions A and B, we write "A $\lesssim$ B" if $B \le CA$ for some generic constant C that depends only on the shape regularity of the triangulation.

Given any $v \in H^1(\Omega)$, set $Jv \in P_1(\mathcal{T}) \cap C^0(\overline{\Omega})$ similar to [3] by

$$Jv := \sum_{z \in \mathcal{N}} v_z \varphi_z \quad \text{with} \quad v_z := \int_\Omega v\varphi_z \, dx \Big/ \int_\Omega \varphi_z \, dx \in \mathbb{R}.$$

Given $f \in L^2(\Omega)$, let $\operatorname{osc}(f, \mathcal{N}) := \left(\sum_{z \in \mathcal{N}} h_z^2 \min_{f_z \in \mathbb{R}} \|f - f_z\|^2_{L^2(\omega_z)}\right)^{1/2}$.

Lemma 2.1. *For $f \in L^2(\Omega)$ and $v \in H^1(\Omega)$, it holds*

$$\int_\Omega (Jf)v\,dx = \int_\Omega f(Jv)\,dx \qquad \text{and} \qquad \int_\Omega f(v - Jv)\,dx \lesssim \operatorname{osc}(f, \mathcal{N})|||v|||.$$

Proof. The first assertion follows from a direct calculation as in [3]. For the proof of the second assertion, we refer to [25, 26]. ∎

Theorem 2.2 ([27]). *Assume that $u_D \in H^1(\Gamma_D) \cap C^0(\Gamma_D)$ satisfies $u_D \in H^2(E)$ for all $E \in \mathcal{E}(\Gamma_D)$ with the edgewise second partial derivative $\partial^2_{\mathcal{E}} u_D/\partial s^2$ of u_D along Γ_D and let $\mathcal{I}u_D = \sum_{z\in\mathcal{N}(\Gamma_D)} u_D(z)\varphi_z$ denote the nodal interpolation of u_D. Then there exists $w_D \in H^1(\Omega)$ with*

$$\begin{aligned} w_D|_{\Gamma_D} &= u_D|_{\Gamma_D} - \mathcal{I}u_D|_{\Gamma_D}, \\ \operatorname{supp}(w_D) &\subset \bigcup\{T \in \mathcal{T} | T \cap \Gamma_D \neq \varnothing\}, \\ \|w_D\|_{L^\infty(\Omega)} &= \|u_D - \mathcal{I}u_D\|_{L^\infty(\Gamma_D)}, \\ |||w_D||| &\lesssim \left\| h_{\mathcal{E}}^{3/2} \partial^2_{\mathcal{E}} u_D/\partial s^2 \right\|_{L^2(\Gamma_D)}. \end{aligned}$$

Furthermore, if $\chi \le \mathcal{I}\chi \le u_D$ it holds

$$\chi - u_h \le w_D.$$

Proof. The inequality $\chi - u_h \le w_D$ is an immediate consequence of the design in [27] with $\chi - u_h \le \mathcal{I}\chi - u_h \le u_D - \mathcal{I}u_D = w_D$ on $E \subset \Gamma_D$ and $(\mathcal{I}\chi)(\operatorname{mid}(T)) - u_h(\operatorname{mid}(T)) \le 0 = w_D(\operatorname{mid}(T))$ plus the linearity of w_D and $\mathcal{I}\chi - u_h$ along the lines that connect the boundary points on E with $\operatorname{mid}(T)$. The remaining details are contained in [27]. ∎

III. RELIABLE ERROR ESTIMATION

This section is devoted to the design of reliable error estimators for the Poisson problem (1.5) with some function Λ_h. Subsections A-C of section III introduce Λ_h in three steps from a postprocessed Riesz representation of a residual similar to [3, 6].

A. Residuals

The exact solution u of (1.1) defines the residual functional

$$\sigma := F - a(u, \cdot) \in V^\star := \text{dual of } V. \tag{3.1}$$

The discrete solution u_h of (1.4) defines the discrete residual functional

$$\sigma_h := F - a(u_h, \cdot) \in V(\mathcal{T})^\star \tag{3.2}$$

with the test function space $V(\mathcal{T}) := P_1(\mathcal{T}) \cap V$. The two properties (3.3) and (3.4) are important in the sequel. The discrete complementary conditions read

$$(u_h(z) - \mathcal{I}\chi(z))\sigma_h(\varphi_z) = 0 \quad \text{and} \quad \sigma_h(\varphi_z) \le 0 \quad \text{for all } z \in \mathcal{M}. \tag{3.3}$$

For $w_D \in H^1(\Omega)$ with $w_D = u_D - \mathcal{I}u_D$ on Γ_D and $\chi - u_h \le w_D$ in Ω, it holds

$$0 \le \sigma(e - w_D). \tag{3.4}$$

B. Boundary Modifications

The complementary conditions (3.3) state that $\sigma_h \in V(\mathcal{T})^\star$ contains information about the contact zone $\{u_h = \mathcal{I}\chi\}$. That information will be used to define some contact force on the entire domain. However, we have to define σ_h also at Dirichlet nodes. Veeser mentioned that $\sigma_h = 0$ on Γ_D may lead to big refinement indicators [8, p. 153 line 25]. Our own numerical experiments confirm this observation. Here we avoid to enforce $\sigma_h|_{\Gamma_D} = 0$ by extrapolation of the known contact information as follows.

For each fixed node $z \in \mathcal{N}\backslash\mathcal{M}$, we choose a neighboring free node $\zeta(z) \in \mathcal{M}$ and set $\zeta(z) := z$ for $z \in \mathcal{M}$. In Section IV, we assume that $\zeta(y) \in \overline{\omega}_T$ for all $y \in \mathcal{N}$ and that every triangle has a free node. The proof of efficiency will make use of this further assumption, but it is not needed for the proof of reliability at the end of Section III.

The mapping ζ defines a partition of $\mathcal{N}$into card$(\mathcal{M})$ many classes

$$\zeta^{-1}(z) := \{y \in \mathcal{N} | \zeta(y) = z\} \text{ for each } z \in \mathcal{M}.$$

For each $z \in \mathcal{M}$ set

$$\psi_z := \sum_{y \in \zeta^{-1}(z)} \varphi_y \in P_1(\mathcal{T}) \cap C^0(\Omega). \tag{3.5}$$

Notice that $(\psi_z | z \in \mathcal{M})$is a partition of unity [25]. For each $z \in \mathcal{N}$ set

$$\widehat{\sigma}_h(\varphi_z) := \begin{cases} 0 & \text{if } \chi(z) < u_h(z), \\ \sigma_h(\varphi_{\zeta(z)}) \frac{\int_\Omega \varphi_z \, dx}{\int_\Omega \varphi_{\zeta(z)} \, dx} & \text{else.} \end{cases} \tag{3.6}$$

A direct consequence of (3.3) is

$$\sum_{z \in \mathcal{N}} \frac{\widehat{\sigma}_h(\varphi_z)}{\int_\Omega \varphi_z \, dx} \varphi_z \le 0. \tag{3.7}$$

Remark 3.1. *Veeser* [8] *suggests the alternative boundary modification with*

$$\widehat{\sigma}_h(\varphi_z) := \begin{cases} 0 & \text{if } \chi(z) < u_h(z), \\ \min\{0, F(\varphi_z) - a(u_h, \varphi_z) + \int_{\Gamma_D} \varphi_z \nabla u_h \cdot \nu \, \mathrm{ds}\} & \text{else.} \end{cases}$$

This resembles the original definition of the residual with an additional boundary term where ν denotes the outer unit normal along $\partial\Omega$.

C. Riesz Representation and Auxiliary Problem

The Riesz representation $\Lambda_h \in P_1(\mathcal{T}) \cap C^0(\Omega)$ of the extended $\widehat{\sigma}_h \in (P_1(\mathcal{T}) \cap C^0(\Omega))^\star$ from (3.6) in the Hilbert space $L^2(\Omega)$ satisfies

$$\int_\Omega \Lambda_h \varphi_z \, dx = \widehat{\sigma}_h(\varphi_z) \quad \text{for all} \quad z \in \mathcal{N}. \tag{3.8}$$

This defines the auxiliary problem (1.5) from the introduction section: Seek $w \in \mathcal{I}u_D + V$ with

$$a(w, v) = F(v) - \int_\Omega \Lambda_h v \, dx \quad \text{for all} \quad v \in V. \tag{3.9}$$

In view of (3.8), the discrete solution u_h of (1.4) equals the finite element approximation of the exact solution w of (3.9). The residual (3.1) of the exact problem also defines some Riesz representation $\Lambda \in L^2(\Omega)$ with

$$\int_\Omega \Lambda v \, dx = \sigma(v) \text{ for all } v \in V. \tag{3.10}$$

D. Main Result

The view of Braess onto the obstacle problem at hand leads to the following reliable error estimate

$$|||u - u_h||| \le |||w - u_h||| + |||\Lambda_h - J\Lambda_h|||_* + \left(\int_\Omega (\chi - u_h - w_D) J\Lambda_h \, dx \right)^{1/2} + 2|||w_D|||$$

The following result is slightly sharper and uses

$$a := |||w - u_h||| + |||\Lambda_h - J\Lambda_h|||_* + |||w_D||| \quad \text{and} \quad b := \int_\Omega (\chi - u_h - w_D) J\Lambda_h \, dx \, .$$

Theorem 3.2. *Let u denote the exact solution of* (1.1) *and let u_h denote the discrete solution of* (1.4) *with the associated Λ_h from* (3.8) *and Λ from* (3.10). *For $\chi \le \mathcal{I}\chi$ and $w_D \in H^1(\Omega)$ with $w_D = u_D - \mathcal{I}u_D$ on Γ_D and $\chi - u_h \le w_D$ in Ω, it holds*

$$|||u - u_h||| \le a/2 + \sqrt{a^2/4 + b} + |||w_D|||,$$
$$|||\Lambda - \Lambda_h|||_* \le |||w - u_h||| + |||u - u_h|||.$$

Some remarks are in order before the proof of Theorem 3.2 concludes this section.

Remark 3.3. *The energy norm $|||w - u_h|||$ of the discretization error in the auxiliary problem equals the dual norm*

$$|||\operatorname{Res}|||_* := \sup_{\substack{v \in V \\ |||v||| = 1}} \operatorname{Res}(v)$$

of the residual $\operatorname{Res} \in V^\star$ *defined, for $v \in V$, by*

$$\operatorname{Res}(v) := \int_\Omega (f - \Lambda_h) v \, dx + \int_{\Gamma_N} g v \, ds - a(u_h, v).$$

(The Riesz representation theorem in the Hilbert space (V, a) yields direct proof, cf. [28] *for details.) The substitute of $|||w - u_h||| = |||\operatorname{Res}|||_*$ and $V_h \subseteq \ker(\operatorname{Res})$ allows an interpretation of the a posteriori error control in Theorem 3.2 in the spirit of the unified approach* [29]. *In fact, all error estimators of* [29, 30] *apply to the control of $|||\operatorname{Res}|||_*$.*

Remark 3.4. *The term* $\int_\Omega(\chi - u_h - w_D)J\Lambda_h\,dx$ *can be evaluated exactly (up to quadrature errors). In case* $\chi = \mathcal{I}\chi$*, this term only contributes on a layer between the discrete contact zone and the discrete noncontact zone* $\{T \in \mathcal{T} | \exists z, y \in \mathcal{N}(T),\ \chi(z) < u_h(z)\ \&\ \widehat{\sigma}_h(\varphi_y) < 0\}$.

Remark 3.5. *The properties of* w_D *from Theorem 2.2 guarantee that the term* $|||w_D|||$ *is bounded by the higher-order term*

$$|||w_D||| \lesssim \left\| h_{\mathcal{E}}^{3/2}\partial_{\mathcal{E}}^2 u_D/\partial s^2 \right\|_{L^2(\Gamma_D)}.$$

For triangulations that consists only of right isosceles triangles along the Dirichlet boundary, the constant in this estimate equals one. This will be proven in [31]. *Furthermore,* w_D *contributes to* $\int_\Omega(\chi - u_h - w_D)J\Lambda_h\,dx$ *only on elements with contact near the boundary. For homogeneous Dirichlet data,* $w_D \equiv 0$.

Remark 3.6. *Theorem 3.2 implies the reliable upper bound*

$$|||\Lambda - \Lambda_h|||_* \le 2|||w - u_h||| + |||\Lambda_h - J\Lambda_h|||_* + \left(\int_\Omega(\chi - u_h - w_D)J\Lambda_h\,dx\right)^{1/2} + 2|||w_D|||.$$

Remark 3.7. *As a conclusion, for the estimation of* $|||u - u_h|||$ *or* $|||\Lambda - \Lambda_h|||_*$ *it remains to estimate* $|||w - u_h|||$. *This can be done with any a posteriori estimator known for Poisson problems, collected in* [23, 24].

Proof of Theorem 3.2. The proof is similar to the proof of Lemma 3.1 in [6] for $\sigma_h^+ := -J\Lambda_h$. Indeed, for $v \in V$, (3.1) and (3.9) imply

$$a(u - w, v) = \int_\Omega v\Lambda_h\,dx - \sigma(v) = \int_\Omega vJ\Lambda_h\,dx - \sigma(v) + \int_\Omega v(\Lambda_h - J\Lambda_h)\,dx\,.$$

For $v := u - u_h - w_D = e - w_D \in V$, it holds

$$\begin{aligned}&\int_\Omega(u - u_h - w_D)J\Lambda_h\,dx - \sigma(e - w_D)\\ &= \int_\Omega(\chi - u_h - w_D)J\Lambda_h\,dx - \int_\Omega(\chi - u)J\Lambda_h\,dx\, - \sigma(e - w_D).\end{aligned}$$

The properties (3.4), $\chi - u \le 0$, and $J\Lambda_h \le 0$ from (3.7) yield

$$0 \le \int_\Omega(\chi - u)J\Lambda_h\,dx \quad \text{and} \quad 0 \le \sigma(e - w_D).$$

Hence

$$\int_\Omega(u - u_h - w_D)J\Lambda_h\,dx - \sigma(e - w_D) \le \int_\Omega(\chi - u_h - w_D)J\Lambda_h\,dx\,.$$

The combination of the previous equality and inequality with some algebra leads to

$$\begin{aligned}&|||u - u_h - w_D|||^2\\ &= a(u - w, u - u_h - w_D) + a(w - u_h, u - u_h - w_D) - a(w_D, u - u_h - w_D)\\ &\le (|||w - u_h||| + |||\Lambda_h - J\Lambda_h|||_* + |||w_D|||)|||u - u_h - w_D||| + \int_\Omega(\chi - u_h - w_D)J\Lambda_h\,dx\,.\end{aligned}$$

This is an inequality of the form $x^2 \leq ax + b$ and Braess reasonably concludes $x \leq a + b^{1/2}$. Since we are interested in sharp estimates, we deduce

$$0 \leq x \leq a/2 + \sqrt{a^2/4 + b}.$$

This and the triangle inequality

$$|||u - u_h||| \leq |||u - u_h - w_D||| + |||w_D|||$$

prove the first assertion. Furthermore, (3.1) and (3.9) yield

$$\int_\Omega (\Lambda - \Lambda_h) v \, dx = a(u - w, v) \leq |||u - w||| |||v||| \text{ for all } v \in V.$$

Hence,

$$|||\Lambda - \Lambda_h|||_* \leq |||u - w|||.$$

The triangle inequality concludes the proof for the second assertion. ∎

IV. EFFICIENCY

This section discusses the efficiency of the GUB and involves some notation $\mathcal{T}_{DC}$, $\mathcal{T}_C$, $\mathcal{T}_i$, Ω_1, Ω_2 as follows. The set of all triangles $T \in \mathcal{T}$ along the Dirichlet boundary Γ_D with contact of the discrete solution on the neighborhood $\omega_T := \{K \in \mathcal{T} | T \cap K \neq \varnothing\} \subseteq \{u_h = \mathcal{I}\chi\}$ is denoted by

$$\mathcal{T}_{DC} := \{T \in \mathcal{T} | \mathcal{E}(T) \cap \mathcal{E}(\Gamma_D) \neq \varnothing \text{ and } u_h = \mathcal{I}\chi \text{ on } \omega_T\}.$$

The set of all triangles T with contact of the discrete solution $\{u_h = \mathcal{I}\chi\}$ is denoted by

$$\mathcal{T}_C := \{T \in \mathcal{T} | u_h = \mathcal{I}\chi \text{ on } T\}.$$

The set of all triangles T in some layer between $\mathcal{T}_{DC} \cup \mathcal{T}_C$ and the set $\{\mathcal{I}\chi \leq u_h\}$ is denoted by

$$\mathcal{T}_i := \{T \in \mathcal{T} | \exists x, y \in \mathcal{N}(\overline{\omega}_T),\ \mathcal{I}\chi(x) = u_h(x) \ \&\ \mathcal{I}\chi(y) < u_h(y)\}.$$

Here, $\mathcal{N}(\overline{\omega}_T) := \{z \in \mathcal{N} | z \in \overline{\omega}_T\}$ denotes all nodes in the element patch ω_T of the triangle T. With each $T \in \mathcal{T}_i$ we associate some (preferably interior) node $z_T \in \mathcal{N} \cap \overline{\omega}_T$ such that $\chi(z_T) = u_h(z_T)$ and set $\widehat{\Omega}_{z_T} := \{x \in \Omega | x \in \omega_T \text{ or } \psi_{z_T}(x) > 0\}$. All elements $T \in \mathcal{T}_i$ with $z_T \in \Gamma_N$ form the set

$$\mathcal{T}_N := \{T \in \mathcal{T}_i | z_T \in \Gamma_N\}$$

and the L^2-norm over all triangles in $\mathcal{T}_N$ reads $\| \cdot \|_{L^2(\mathcal{T}_N)}$.

The next theorem establishes efficiency for the GUB

$$\text{GUB} := 3|||w - u_h||| + 2|||\Lambda_h - J\Lambda_h|||_* + 2\left(\int_\Omega (\chi - u_h - w_D) J\Lambda_h \, dx\right)^{1/2} + 4|||w_D|||$$

from Theorem 3.2. This is the converse of

$$|||u - u_h||| + |||\Lambda - \Lambda_h|||_* \leq \text{GUB}$$

up to pertubation terms like oscillations with respect to node patches $\operatorname{osc}(\Lambda,\mathcal{N})$ and elementwise or edgewise oscillations defined by

$$\operatorname{osc}(f,\mathcal{T}) := \|h_{\mathcal{T}}(f-f_{\mathcal{T}})\|_{L^2(\Omega)}, \quad \operatorname{osc}(g,\mathcal{E}(\Gamma_N)) := \|h_{\mathcal{E}}(g-g_{\mathcal{E}})\|_{L^2(\Gamma_N)}$$

with elementwise integral mean $f_{\mathcal{T}}|_T := \int_T f\,dx/|T|$ and edgewise integral mean $g_{\mathcal{E}}|_E := \int_E g\,\mathrm{ds}/|E|$.

Theorem 4.1. *For an affine obstacle $\chi = \mathcal{I}\chi \in P_1(\Omega)$ and $f \in H^1(\Omega)$, it holds*

$$\mathrm{GUB} \lesssim |\!|\!| u-u_h |\!|\!| + |\!|\!| \Lambda - \Lambda_h |\!|\!|_* + \operatorname{osc}(\Lambda,\mathcal{N}) + \operatorname{osc}(f,\mathcal{T}) + \operatorname{osc}(g,\mathcal{E}(\Gamma_N)) + |\!|\!| w_D |\!|\!|$$
$$+ \left(\sum_{T\in\mathcal{T}_i\setminus\mathcal{T}_C} \left\| h_{\mathcal{T}}^2 \nabla f \right\|_{L^2(\omega_T)}^2 \right)^{1/2} + \left(\sum_{T\in\mathcal{T}_{DC}} \|\nabla w_D\|_{L^2(T)} \|h_{\mathcal{T}} f\|_{L^2(T)} \right)^{1/2} + \|\nabla(u-\chi)\|_{L^2(\mathcal{T}_N)}.$$

Proof. The proof of Theorem 4.1 follows by a combination of Claim 1 - Claim 6 below. ∎

Claim 1. It holds $|\!|\!| w-u_h |\!|\!| \le |\!|\!| u-u_h |\!|\!| + |\!|\!| \Lambda - \Lambda_h |\!|\!|_*$.

Proof of Claim 1. This is already known from [6]. ∎

Claim 2. It holds $|\!|\!| J\Lambda_h - \Lambda_h |\!|\!|_* \lesssim |\!|\!| \Lambda_h - \Lambda |\!|\!|_* + \operatorname{osc}(\Lambda,\mathcal{N})$.

Proof of Claim 2. For any $v \in V$, Lemma 2.1 shows that

$$\int_\Omega (J\Lambda_h) v\,dx = \int_\Omega \Lambda_h J v\,dx\,.$$

This and the second assertion of Lemma 2.1 lead to

$$\begin{aligned}\int_\Omega (\Lambda_h - J\Lambda_h) v\,dx &= \int_\Omega (\Lambda_h-\Lambda)(v-Jv)\,dx + \int_\Omega \Lambda(v-Jv)\,dx \\ &\lesssim |\!|\!| v |\!|\!| (|\!|\!| \Lambda_h - \Lambda |\!|\!|_* + \operatorname{osc}(\Lambda,\mathcal{N})).\end{aligned}$$

∎

Claim 3. It holds

$$\begin{aligned}&\int_\Omega (\chi - u_h - w_D)(J\Lambda_h)\,dx \\ &\lesssim \sum_{T\in\mathcal{T}_{DC}} h_T \|\nabla w_D\|_{L^2(T)} \|J\Lambda_h\|_{L^2(T)} + \sum_{T\in\mathcal{T}_i\setminus\mathcal{T}_{DC}} h_T^2 \|\nabla w_D\|_{L^2(T)} \|\nabla(J\Lambda_h)\|_{L^2(\omega_T)} \\ &+ \sum_{T\in\mathcal{T}_i\setminus\mathcal{T}_C} h_T^2 \|\nabla(J\Lambda_h)\|_{L^2(\omega_T)} \min_{q_z\in(P_1(\mathcal{T}(\widehat{\Omega}_{z_T}))\cap C(\widehat{\Omega}_{z_T}))^2} \|\nabla(\chi-u_h) - q_z\|_{L^2(\widehat{\Omega}_{z_T})}.\end{aligned}$$

The proof of Claim 3 employs Lemma 8 of [3] which is recalled here for convenient reading.

Lemma 4.2 ([3]). *Let $z \in \mathcal{N}$ be either an interior point of Ω or a nonconvex boundary point (so convex corner, in particular points on straight line segments are excluded). Suppose $T \in \mathcal{T}$, $\omega_T := \{\sum_{z\in\mathcal{N}(T)} \varphi_z > 0\}$ with $z \in \overline{\omega}_T$ and set $\widehat{\Omega}_z := \{x \in \Omega | \psi_z(x) > 0\} \cup \omega_T$. Let $w_h \in P_1(\mathcal{T}) \cap C(\Omega)$ satisfy $w_h(z) = 0$ and $0 \le w_h$ on $\widehat{\Omega}_z$. Then, it holds*

$$\|w_h\|_{L^2(\widehat{\Omega}_z)} \lesssim h_z \min_{q_z \in \left(P_1(\mathcal{T}(\widehat{\Omega}_z))\cap C(\widehat{\Omega}_z)\right)^2} \|\nabla w_h - q_z\|_{L^2(\widehat{\Omega}_z)}.$$

Proof of Claim 3. The integral $\int_\Omega (\chi - u_h - w_D)(J\Lambda_h)\,dx$ is analyzed for each $T \in \mathcal{T}$. In case that $\chi < u_h$ on $\overline{\omega}_T$, (3.3) yields

$$J\Lambda_h = \sum_{z\in\mathcal{N}(T)} \varphi_z \widehat{\sigma}_h(\varphi_z) \Big/ \int_\Omega \varphi_z\,dx = 0 \quad \text{on } T.$$

For $T \in \mathcal{T}_i \backslash \mathcal{T}_C$ with $|\partial T \cap \Gamma_D| = 0$, it holds $w_D = 0$ on T and $(u_h - \chi)(z_T) = 0$ for some $z_T \in \mathcal{N}(\overline{\omega}_T)$. Furthermore, there exists some $y_T \in \mathcal{N}(T)$ with $\chi(y_T) < u_h(y_T)$. Since (3.6) and (3.3) yield

$$J\Lambda_h(y_T) = \widehat{\sigma}_h(y_T) \Big/ \int \varphi_{y_T}\,dx = 0,$$

a discrete Friedrichs' inequality shows

$$\|J\Lambda_h\|_{L^2(T)} \lesssim h_T \|\nabla(J\Lambda_h)\|_{L^2(\omega_T)}. \tag{4.1}$$

This and Lemma 4.2 yield

$$\begin{aligned}\int_T (\chi - u_h)(J\Lambda_h)\,dx &\le \|\chi - u_h\|_{L^2(T)} \|J\Lambda_h\|_{L^2(T)} \\ &\lesssim h_T^2 \|\nabla(J\Lambda_h)\|_{L^2(\omega_T)} \min_{q_z \in (P_1(\mathcal{T}(\widehat{\Omega}_{z_T}))\cap C(\widehat{\Omega}_{z_T}))^2} \|\nabla(\chi - u_h) - q_z\|_{L^2(\widehat{\Omega}_{z_T})}.\end{aligned}$$

If $z_T \in \Gamma_D$, Lemma 4.2 is not applicable. However, this case is insignificant for the following reason. Since z_T is chosen preferably as an inner node, $z_T \in \Gamma_D$ implies $\mathcal{N}(\overline{\omega}_z) \cap \{u_h = \mathcal{I}\chi\} \subseteq \mathcal{N}(\Gamma_D)$. Hence $\widehat{\sigma}_h(y) = 0$ for all $y \in \mathcal{N}(T)$. Consequently, $J\Lambda_h = 0$ on T. In case that the isolated contact node z_T belongs to a convex corner or a straight-line segment of Γ_N, it follows that

$$\int_T (\chi - u_h)(J\Lambda_h)\,dx \le h_T^2 \|\nabla(\chi - u_h)\|_{L^2(T)} \|J\Lambda_h\|_{L^2(T)}.$$

In fact, free nodes on convex corners lead to exceptional situations in some second-order positive approximation [32].

For $T \in \mathcal{T}$ with $|\partial T \cap \Gamma_D| > 0$ the integral equals

$$\begin{aligned}\int_T (\chi - u_h - w_D)(J\Lambda_h)\,dx &= \int_T (\chi - u_h)(J\Lambda_h)\,dx - \int_T w_D(J\Lambda_h)\,dx \\ &\le \|\chi - u_h\|_{L^2(T)} \|J\Lambda_h\|_{L^2(T)} + \|w_D\|_{L^2(T)} \|J\Lambda_h\|_{L^2(T)}.\end{aligned}$$

Since $w_D = 0$ on $\partial T \backslash \Gamma_D$, a Friedrichs inequality shows

$$\int_T (\chi - u_h - w_D)(J\Lambda_h)\,dx \lesssim \|\chi - u_h\|_{L^2(T)} \|J\Lambda_h\|_{L^2(T)} + h_T \|\nabla w_D\|_{L^2(T)} \|J\Lambda_h\|_{L^2(T)}.$$

The first summand vanishes if $u_h = \chi$ on T or $\chi < u_h$ on ω_T. Otherwise, it holds $T \in \mathcal{T}_i$ and Lemma 4.2 leads for $z = z_T \in \mathcal{N}(\Omega)$ to

$$\|\chi - u_h\|_{L^2(\widehat{\Omega}_z)} \lesssim h_{z_T} \min_{q \in (P^1(\mathcal{T}(\widehat{\Omega}_{z_T})) \cap C(\widehat{\Omega}_{z_T}))^2} \|\nabla(\chi - u_h) - q\|_{L^2(\widehat{\Omega}_{z_T})}.$$

The factor $\|J\Lambda_h\|_{L^2(T)}$ can be treated as in (4.1), except in case $u_h = \chi$ on ω_T which implies $T \in \mathcal{T}_{DC}$. ∎

Claim 4. For any $T \in \mathcal{T}$, it holds

$$\begin{aligned} h_T \|J\Lambda_h\|_{L^2(T)} &\lesssim h_T \|f\|_{L^2(\omega_T)} \\ &\quad + \min_{q_T \in (P_1(\mathcal{T}(\omega_T)) \cap C(\omega_T))^2} \big(\|\nabla u_h - q_T\|_{L^2(\omega_T)} + h_T^{1/2} \|(g - q_T \cdot \nu)\|_{L^2(\Gamma_N \cap \partial\omega_T)} \big), \qquad (4.2) \\ h_T^2 \|\nabla(J\Lambda_h)\|_{L^2(T)} &\lesssim h_T^2 \|\nabla f\|_{L^2(\omega_T)} \\ &\quad + \min_{q_T \in (P_1(\mathcal{T}(\omega_T)) \cap C(\omega_T))^2} \big(\|\nabla u_h - q_T\|_{L^2(\omega_T)} + h_T^{1/2} \|(g - q_T \cdot \nu)\|_{L^2(\Gamma_N \cap \partial\omega_T)} \big). \qquad (4.3) \end{aligned}$$

Proof of Claim 4. Since $J\Lambda_h = \varrho_h$, this is Lemma 7 in [3]. ∎

Claim 5. It holds

$$\begin{aligned} &\min_{q_T \in (P_1(\mathcal{T}(\omega_T)) \cap C(\omega_T))^2} \big(\|\nabla u_h - q_T\|^2_{L^2(\omega_T)} + h_T \|g - q_E \cdot \nu\|^2_{L^2(\Gamma_N \cap \partial\omega_T)} \big) \\ &\lesssim \sum_{E \in \mathcal{E}(\omega_T)} \min_{q_E \in (P_1(\mathcal{T}(\omega_E)) \cap C(\omega_T))^2} \big(\|\nabla u_h - q_E\|^2_{L^2(\omega_E)} + h_T \|g - q_E \cdot \nu\|^2_{L^2(\Gamma_N \cap E)} \big) \\ &\lesssim \sum_{E \in \mathcal{E}(\omega_T)} h_E \|[\nabla u_h \cdot \nu]\|^2_{L^2(E)} + \sum_{E \in \mathcal{E}(\Gamma_N)} h_E \|g - \nabla u_h \cdot \nu\|^2_{L^2(\Gamma_N \cap E)}, \\ &\min_{q_z \in (P_1(\mathcal{T}(\widehat{\Omega}_{z_T})) \cap C(\widehat{\Omega}_{z_T}))^2} \|\nabla(\chi - u_h) - q_z\|_{L^2(\widehat{\Omega}_{z_T})} \lesssim \sum_{E \in \mathcal{E}(\Omega_{z_T})} h_E \|[\nabla(\chi - u_h) \cdot \nu]\|^2_{L^2(E)}. \end{aligned}$$

Proof of Claim 5. The first estimate follows from (3.4) in [33, p. 951]. Consider an inner edge $E \in \mathcal{E}(\Omega)$ and set $q_E := (\nabla u_h|_{T_1} - \nabla u_h|_{T_2})/2$. This yields

$$\|\nabla u_h - q_E\|^2_{L^2(\omega_E)} = 1/4 \|[\nabla u_h \cdot \nu]\|^2_{L^2(\omega_E)} = |\omega_E|/(4|E|)\, \|[\nabla u_h \cdot \nu]\|^2_{L^2(E)}.$$

For any Neumann edge $E \in \mathcal{E}(\Gamma_N)$, ω_E consists of only one element T and we can set $q_E := \nabla u_h|_T$. This proves the second asserted estimate. ∎

Claim 6. It holds

$$h_T\|f_{\mathcal{T}}+\Lambda_h\|_{L^2(T)}\lesssim\|\nabla(w-u_h)\|_{L^2(T)}+\operatorname{osc}(f,T)\quad\text{for all } T\in\mathcal{T},$$

$$h_E^{1/2}\|[\nabla u_h\cdot\nu]\|_{L^2(E)}\lesssim\|\nabla(w-u_h)\|_{L^2(\omega_E)}+\operatorname{osc}(f,\mathcal{T}(\omega_E))\quad\text{for all } E\in\mathcal{E}(\Omega),$$

$$h_E^{1/2}\|\nabla u_h\cdot\nu-g\|_{L^2(E)}\lesssim\|\nabla(w-u_h)\|_{L^2(T_E)}+\operatorname{osc}(f,T_E)+\operatorname{osc}(g,E)\quad\text{for all } E\in\mathcal{E}(\Gamma_N).$$

Proof of Claim 6. Those estimates are well-known and follow from an error analysis for the explicit residual-based error estimator for Poisson problems with bubble functions [18, 22]. ∎

This section concludes with some remarks in order to support our claim that in model examples —such as the benchmarks below— GUB is equivalent to $|||u-u_h|||+|||\Lambda-\Lambda_h|||_*$ up to higher-order terms.

Remark 4.3 (Comment on $\operatorname{osc}(\Lambda,\mathcal{N})$). *Since Λ is merely an $L^2(\Omega)$ function, it is not clear a priori that the term $\operatorname{osc}(\Lambda,\mathcal{N})$ is of higher order. Consider the maximal open set $\mathcal{C}$ with $u=\chi$ on $\mathcal{C}$ and the set $\mathcal{U}:=\bigcup_{\varepsilon>0}B_\varepsilon$ with the maximal open set B_ε with $\chi+\varepsilon\le u$ on B_ε. Then,*

$$\Lambda=0\ \text{on}\ \mathcal{U}\quad\text{and}\quad\Lambda=f\ \text{on}\ \mathcal{C}.$$

The set $\mathcal{C}$ is regarded as the set of contact and the set $\mathcal{U}$ is the set of noncontact. Hence, the oscillations of Λ on $\mathcal{C}\cup\mathcal{U}$ are bounded by the oscillations of f, while the contributions of Λ within the free boundary $\mathcal{F}:=\Omega\backslash(\mathcal{C}\cup\mathcal{U})$ may be not because of discontinuities.

Remark 4.4 (Heuristic analysis on $\operatorname{osc}(\Lambda,\mathcal{N})=$ higher-order term). *In simple model scenarios, the free boundary $\mathcal{F}$ is indeed a one-dimensional submanifold, cf. Examples 1-3 below, where Λ is piecewise smooth and bounded. Therefore, we expect*

$$\min_{\Lambda_z\in\mathbb{R}}\|\Lambda-\Lambda_z\|^2_{L^2(\omega_z)}\approx|\omega_z|$$

close to the free boundary while it is of higher order elsewhere. For the local mesh-size $h(s)$ along the parametrization of the curve $\mathcal{F}$ by arc-length $0\le s\le L:=|\gamma|\lesssim 1$, it holds $|\omega_z|\approx h(s)^2$ near any point $\gamma(s)\in\omega_z$. The node patches

$$\mathcal{N}(\mathcal{F}):=\{z\in\mathcal{N}|\omega_z\cap\mathcal{F}\neq\varnothing\}$$

along $\mathcal{F}$ are coupled with $J:=|\mathcal{N}(\mathcal{F})|+1$ many points $\gamma(t_0),\dots,\gamma(t_J)$, along γ with $0=t_0<t_1<\ldots<t_J=L$. The nonsmooth contributions $\operatorname{osc}(\Lambda,\mathcal{N}(\mathcal{F}))$ of $\operatorname{osc}(\Lambda,\mathcal{N})$ in the neighborhood of γ sum up to

$$\sum_{z\in\mathcal{N}(\mathcal{F})}h_z^2\min_{\Lambda_z\in\mathbb{R}}\|\Lambda-\Lambda_z\|^2_{L^2(\omega_z)}\lesssim\sum_{j=0}^{J}h(t_j)^4\lesssim\sum_{j=0}^{J}h(t_j)^3(t_{j+1}-t_j)\quad(\text{with } t_{J+1}:=L+h(L))$$

$$=\int_0^L h(s)^3\,\mathrm{d}s\le L\,h_{\max}^3\lesssim h_{\max}^3.$$

TABLE I. Classes of a posteriori error estimators used in this article.

No	Classes of error estimators	Class representatives
1	Explicit residual-based	η_{R}
2	Averaging	η_{MP1}
3	Equilibration	η_{B}, η_{LW}, η_{EQL}
4	Least-square	η_{LS}
5	Localization	η_{CF}

Here $h_{\max}$ denotes the maximal mesh-size along γ which is relatively small compared with the maximal mesh-size $\max_{T\in\mathcal{T}} h_T$ of the triangulation $\mathcal{T}$ for all the adaptive meshes in the numerical examples of Section VI. Therefore,

$$\operatorname{osc}(\Lambda, \mathcal{N}(\mathcal{F})) \lesssim h_{\max}^{3/2}$$

is of higher order compared to $|||u - u_h|||$.

Remark 4.5. *The remaining critical contribution $\|\nabla w_D\|_{L^2(T)}\|h_{\mathcal{T}} f\|_{L^2(T)}$ arises only for a relatively small number of triangles along the Dirichlet boundary. It vanishes for boundary triangles $T \notin \mathcal{T}_{DC}$ without contact at the Dirichlet boundary. It also vanishes for piecewise affine Dirichlet data u_D.*

Remark 4.6. *The contribution $\|\nabla(u - \chi)\|_{L^2(\mathcal{T}_N)}$ vanishes for pure Dirichlet boundary problems with $\Gamma_N = \varnothing$. This is valid for all our benchmark examples in Section VI. It also vanishes for triangles without contact at the Neumann boundary in its neighborhood ω_T.*

V. ERROR ESTIMATION AND ADAPTIVE MESH-REFINEMENT ALGORITHM

This section studies the five classes of a posteriori estimators from Table I and explains our adaptive mesh-refinement algorithm for problems with $\Gamma_D = \partial\Omega$. Modifications for Neumann boundary problems are possible.

A. Five Types of a Posteriori Error Estimators

i. **Explicit residual-based error estimator.** The standard residual estimator

$$\eta_R := \|h_{\mathcal{T}}(f - \Lambda_h)\|_{L^2(\Omega)} + \left(\sum_{E\in\mathcal{E}} h_E \|[\nabla u_h \cdot \nu_E]\|^2_{L^2(E)}\right)^{1/2}$$

is a guaranteed upper bound of $|||w - u_h|||$. In all our examples, $\mathcal{T}$ consists of right isosceles triangles, hence $|||w - u_h||| \le \eta_R$ [34]. Here, $[\nabla u_h \cdot \nu_E]$ denotes the jump of $[\nabla u_h \cdot \nu_E]$ across $E \in \mathcal{E}$, which is set to zero along any Dirichlet edge $E \in \mathcal{E}(\partial\Omega)$.

ii. **Minimal $P_1(\mathcal{T};\mathbb{R}^2)$ averaging** [35]**.** The error estimator

$$\eta_{\mathrm{MP1}} := \min_{q\in P_1(\mathcal{T};\mathbb{R}^2)\cap C(\Omega;\mathbb{R}^2)} \|\nabla u_h - q\|_{L^2(\Omega)}$$

shows very accurate results for the Laplace equation but only yields an upper bound for $|||w - u_h|||$ up to some not-displayed reliability constant $C_{\rm rel}$.

iii. **Least-square estimator.** An integration by parts yields, for any $q \in H(\mathrm{div}, \Omega)$ and $\widehat{f} = f - \Lambda_h$ with elementwise integral mean $\widehat{f_{\mathcal{T}}} \in P_0(\mathcal{T})$, that

$$\int_\Omega \nabla(w - u_h) \cdot \nabla v \, dx = \int_\Omega (\widehat{f} - \widehat{f_{\mathcal{T}}}) v \, dx + \int_\Omega (\widehat{f_{\mathcal{T}}} + \mathrm{div}\, q) v \, dx + \int_\Omega (\nabla u_h - q) \cdot \nabla v \, dx .$$

After [19, 20, 24], this results in the error estimator

$$\eta_{\rm LS} := \min_{q \in RT_0(\mathcal{T})} C_F \| \widehat{f_{\mathcal{T}}} + \mathrm{div}\, q \|_{L^2(\Omega)} + \| \nabla u_h - q \|_{L^2(\Omega)} + \mathrm{osc}(\widehat{f}, \mathcal{T})/\pi$$

with (upper bounds of the) Friedrichs' constant $C_F := \sup_{v \in V \setminus \{0\}} \|v\|_{L^2(\Omega)} / |||v|||$. Our interpretation of Repin's variant (without the oscillation split) reads

$$\eta_{\rm Repin} := \min_{q \in RT_0(\mathcal{T})} C_F \| \widehat{f} + \mathrm{div}\, q \|_{L^2(\Omega)} + \| \nabla u_h - q \|_{L^2(\Omega)} + \mathrm{osc}(\widehat{f}, \mathcal{T})/\pi .$$

This paper studies the least-square variant $\eta_{\rm LS}$ rather than Repin's majorant $\eta_{\rm Repin}$ for reasons discussed in [24, subsection 13 of section IV].

iv. **Luce-Wohlmuth error estimator** [21]**.** Luce and Wohlmuth suggest to solve local problems around each node on the dual triangulation $\mathcal{T}^\star$ of $\mathcal{T}$ and compute some equilibrated quantity $q_{\rm LW}$. The dual triangulation $\mathcal{T}^\star$ connects each triangle center $\mathrm{mid}(T)$, $T \in \mathcal{T}$, with the edge midpoints $\mathrm{mid}(\mathcal{E}(T))$ and nodes $\mathcal{N}(T)$ and so divides each triangle $T \in \mathcal{T}$ into 6 subtriangles of area $|T|/6$.

Consider some node $z \in \mathcal{N}(\mathcal{T})$ and its nodal basis function $\varphi_z^\star$ with the fine patch $\omega_z^\star := \{\varphi_z^\star > 0\}$ of the dual triangulation $\mathcal{T}^\star$ and its neighboring triangles $\mathcal{T}^\star(z) := \{T^\star \in \mathcal{T}^\star | z \in \mathcal{N}^\star(T)\}$. Since $\nabla u_h \in P_0(\mathcal{T})$ is continuous along $\partial\omega_z^\star \cap T$ for any $T \in \mathcal{T}$, $q \cdot \nu = \nabla u_h \cdot \nu \in P_0(\mathcal{E}^\star(\partial\omega_z^\star))$ is well-defined on the boundary edges $\mathcal{E}^\star(\partial\omega_z^\star)$ of $\omega_z^\star$. With $f_{T,z} := \int_T (f - \Lambda_h)\varphi_z \, dx / |T^\star|$ and the local spaces

$$Q(\mathcal{T}^\star(z)) := \big\{ \tau_h \in RT_0(\mathcal{T}^\star(z)) | \, \mathrm{div}\, \tau_h|_{T^\star} + f_{T,z} = 0 \text{ on } T^\star \in \mathcal{T}^\star \text{ with } \mathcal{N}^\star(T^\star) \cap \mathcal{N}(T) = \{z\} \text{ and } q \cdot \nu = \nabla u_h \cdot \nu \text{ along } \partial\omega_z^\star \backslash \partial\Omega \big\},$$

the mixed finite element method solves

$$q|_{\omega_z^\star} := \operatorname*{argmin}_{\tau_h \in Q(\mathcal{T}^\star(z))} \| q_h - \tau_h \|_{L^2(\omega_z^\star)}.$$

The choice $f^\star \in P_0(\mathcal{T}^\star)$ with $f^\star|_{T^\star} := f_{T,z}$ on $T^\star \in \mathcal{T}^\star$ with $\mathcal{N}(T) \cap \mathcal{N}^\star(T^\star) = z$ for the divergence differs from the original one of [21], but it also satisfies the local compatibility condition $\int_{\omega_z^\star} f^\star dx = \int_{\partial\omega_z^\star} \nabla u_h \cdot \nu ds$. Since $\int_T (f^\star - f + \Lambda_h) dx = 0$, it allows for an improved bound for $|||f - \Lambda_h + \mathrm{div}\, q_{\rm LW}|||_\star$ with explicitly known constants, namely

$$|||f - \Lambda_h + \mathrm{div}\, q_{\rm LW}|||_\star \le \| h_{\mathcal{T}} (f - \Lambda_h - f^\star) \|_{L^2(\Omega)} / \pi .$$

The remaining degrees of freedom permit proper boundary fluxes and

$$\int_\Omega q_{\rm LW} \cdot \mathrm{Curl} \varphi_z^\star \, dx = \int_\Omega \nabla u_h \cdot \mathrm{Curl} \varphi_z^\star \, dx \qquad \text{for all } z \in \mathcal{N}.$$

Here, Curl denotes the rotated gradient $\mathrm{Curl} v := (-\partial v/\partial x_2, \partial v/\partial x_1)$. Then, the Luce-Wohlmuth error estimator in our preferred modification reads

$$\eta_{\mathrm{LW}} := \|\nabla u_h - q_{\mathrm{LW}}\|_{L^2(\Omega)} + \|h_{\mathcal{T}}(f - \Lambda_h + \operatorname{div} q_{\mathrm{LW}})\|_{L^2(\Omega)}/\pi.$$

v. **Equilibration error estimator by Braess.** Braess [22,36] designs, for every $z \in \mathcal{N}$, broken Raviart-Thomas functions $r_z \in RT_{-1}(\mathcal{T}(z)) := \{q \in L^2(\Omega;\mathbb{R}^2) | \forall T \in \mathcal{T}(z), q|_T \in RT_0(\mathcal{T}(z))\}$ on $\mathcal{T}(z) := \{T \in \mathcal{T} | z \in \mathcal{N}(T)\}$ that satisfy

$$\begin{aligned} \operatorname{div} r_z|_T &= -\int_T (f - \Lambda_h)\varphi_z \, dx \,/|T| && \text{for } T \in \mathcal{T}(z), \\ [r_z \cdot \nu_E]_E &= -[\nabla u_h \cdot \nu_E]_E/2 && \text{on } E \in \mathcal{E}(z) \cap \mathcal{E}(\partial\Omega), \\ r_z \cdot \nu &= 0 && \text{along } \partial\omega_z \backslash \mathcal{E}(\partial\Omega). \end{aligned}$$

The set $\mathcal{E}(z)$ denotes the edges that have $z \in \mathcal{N}$ in common. Eventually, the quantity $q_{\mathrm{B}} := \nabla u_h + \sum_{z\in\mathcal{N}} r_z \in RT_0(\mathcal{T})$ satisfies $\operatorname{div} q_{\mathrm{B}}|_T = -\int_T (f - \Lambda_h)\, dx\,/|T|$ for every $T \in \mathcal{T}$. The resulting error estimator reads

$$\eta_{\mathrm{B}} := \|\nabla u_h - q_{\mathrm{B}}\|_{L^2(\Omega)} + \operatorname{osc}(f - \Lambda_h, \mathcal{T})/\pi.$$

vi. **Equilibration error estimator by Ladeveze.** The fluxes q_L designed by Ladeveze-Leguillon [37] act as Neumann boundary conditions for local problems on each triangle, cf. also [14] for details. Given the local function space $H^1_D(T) := H^1(T)/\mathbb{R}$ if $|T \cap \Gamma_D| = 0$ and $H^1_D(T) := \{v \in H^1(T) | v = 0 \text{ on } \partial T \cap \Gamma_D\}$ otherwise, seek $\phi_T \in H^1_D(T)$ with

$$\int_T \phi_T \cdot \nabla v \, dx = \int_T (f - \Lambda_h) v \, dx - \int_T \nabla u_h \cdot \nabla v \, dx + \int_{\partial T} q_{\mathrm{L}} \cdot \nu_T \, v \, \mathrm{ds}$$

for all $v \in H^1_D(T)$. Then the error estimate reads

$$|||w - u_h||| \le \eta_{\mathrm{EQL}} := \left(\sum_{T\in\mathcal{T}} \|\nabla \phi_T\|^2_{L^2(T)}\right)^{1/2}.$$

vii. **Carstensen-Funken error estimator.** The partition of unity property of the nodal basis functions leads in [34] to the solution of local problems on node patches: For every $z \in \mathcal{N}$ seek

$$w_z \in W_z := \begin{cases} \left\{v \in H^1_{\mathrm{loc}}(\omega_z) \middle| \left\|\varphi_z^{1/2}\nabla v\right\|_{L^2(\omega_z)} < \infty, v = 0 \text{ on } \Gamma_D \cap \partial\omega_z\right\} & \text{if } z \in \overline{\Gamma}_D, \\ \left\{v \in H^1_{\mathrm{loc}}(\omega_z) \middle| \left\|\varphi_z^{1/2}\nabla v\right\|_{L^2(\omega_z)} < \infty\right\}/\mathbb{R} & \text{otherwise} \end{cases}$$

with

$$\int_{\omega_z} \varphi_z \nabla w_z \cdot \nabla v \, dx = \int_{\omega_z} \varphi_z (f - \Lambda_h) v \, dx - \int_{\omega_z} \nabla u_h \cdot \nabla(\varphi_z v) \, dx \quad \text{for all } v \in W_z.$$

Then the error estimator reads

$$|||w - u_h||| \le \eta_{\mathrm{CF}} := \left(\sum_{z\in\mathcal{N}} \left\|\varphi_z^{1/2}\nabla w_z\right\|^2_{L^2(\omega_z)}\right)^{1/2}.$$

In the computations for η_{CF} and η_{EQL}, all the local problems are solved with fourth-order polynomials for simplicity. The computed values are regarded as very good approximations. However, strictly speaking the values displayed for η_{EQL} or η_{CF} are lower bounds of the guaranteed upper bounds.

B. Adaptive Mesh Refinement Algorithm and Notation

This section explains our adaptive mesh refinement algorithm and notation for the global upper bound $\mathrm{GUB}(\eta_{\mathrm{xyz}})$. Throughout this section,

$$|||w_D||| \lesssim \left\| h_{\mathcal{E}}^{3/2} \partial_{\mathcal{E}}^2 u_D / \partial s^2 \right\|_{L^2(\Gamma_D)}$$

denotes the computable upper bound for $|||w_D|||$ from Theorem 2.2. The constant hidden in $\lesssim$ is lower than 1 as proven in [31]. The quantity $|||\Lambda_h - J\Lambda_h|||_*$ is estimated by its upper bound from Lemma 2.1

$$|||\Lambda_h - J\Lambda_h|||_* \lesssim \mathrm{osc}(\Lambda_h, \mathcal{N}) := \left(\sum_{z \in \mathcal{N}} h_z^2 \min_{f_z \in \mathbb{R}} \|\Lambda_h - f_z\|_{L^2(\omega_z)}^2 \right)^{1/2}.$$

In our computations, the constants hidden in $\lesssim$ were set to 1 for simplicity. Moreover, there is the contact-related contribution

$$\mu_h := \left(\int_\Omega (\chi - u_h - w_D) J\Lambda_h \, dx \right)^{1/2}.$$

Automatic mesh refinement generates a sequence of meshes $\mathcal{T}_0$, $\mathcal{T}_1$, $\mathcal{T}_2$,…by succesive mesh refinement according to a bulk criterion with parameter $0 < \Theta \leq 1$.

Algorithm.

INPUT coarse mesh $\mathcal{T}_0$, $0 < \theta \leq 1$. For level $\ell = 0, 1, 2, \ldots$ until termination do

COMPUTE discrete solution $u_h$on $\mathcal{T}_\ell$ (e.g. with the MATLAB routine `quadprog`) and Λ_h from Section III.

ESTIMATE by

$$\begin{aligned} \mathrm{GUB}(\eta_{\mathrm{xyz}}) = {} & (\eta_{\mathrm{xyz}} + \mathrm{osc}(\Lambda_h, \mathcal{N}) + 3|||w_D|||)/2 \\ & + \sqrt{\mu_h^2 + (\eta_{\mathrm{xyz}} + \mathrm{osc}(\Lambda_h, \mathcal{N}) + |||w_D|||)^2} \end{aligned}$$

with η_{xyz} replaced by any of the estimators η_{R}, η_{MP1}, η_{LS}, η_{LW}, η_{EQL}, or η_{CF} from Subsection A of section V.

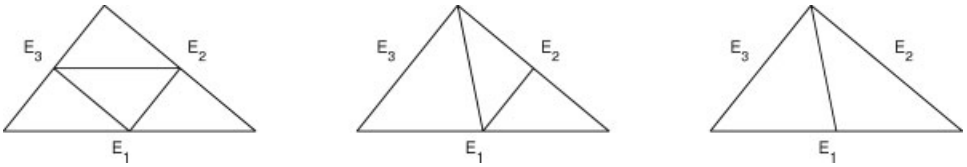

FIG. 1. Red-, blue-, and green-refinement of a triangle.

MARK minimal set $\mathcal{M}_\ell \subseteq \mathcal{T}_\ell$ of elements such that the refinement indicators

$$\eta(T)^2 = |T|\|f - \Lambda_h\|^2_{L^2(T)} + \sum_{E\in\mathcal{E}(T)} |T|^{1/2}\|[\nabla u_h]_E \cdot \nu_E\|^2_{L^2(E)}$$
$$+ \int_T (\chi - u_h - w_D) J\Lambda_h \, dx + \frac{1}{3}\sum_{z\in\mathcal{N}(T)} h_z^2 \min_{f_z\in\mathbb{R}} \|\Lambda_h - J\Lambda_h(z)\|^2_{L^2(\omega_z)}$$
$$+ \sum_{E\in\mathcal{E}(T)\cap\mathcal{E}(\Gamma_D)} h_E^3 \left\|\partial^2_{\mathcal{E}} u_D/\partial s^2\right\|^2_{L^2(E)} \qquad \text{for all } T \in \mathcal{T}_\ell,$$

satisfy

$$\Theta \sum_{T\in\mathcal{T}_\ell} \eta(T)^2 \le \sum_{T\in\mathcal{M}_\ell} \eta(T)^2.$$

REFINE by *red*-refinement of elements in $\mathcal{M}_\ell$ and *red-green-blue*-refinement (Fig. 1) of further elements to avoid hanging nodes and compute $\mathcal{T}_{\ell+1}$.

OUTPUT efficiency index $\mathrm{GUB}(\eta_{\mathrm{xyz}})/|||e|||$ and relative contribution $\eta_{\mathrm{xyz}}/\mathrm{GUB}(\eta_{\mathrm{xyz}})$ for η_{xyz}.

VI. NUMERICAL EXAMPLES

This section studies the five benchmark examples from Table II.

A. Benchmark Example 1

The first benchmark from [5] concerns the constant obstacle $\chi = \mathcal{I}\chi \equiv 0$ on the square domain $\Omega = (-1,1)^2$ subject to smooth Dirichlet data $u_D(r,\varphi) = r^2 - 0.49$ and right-hand side

$$f(r,\varphi) = \begin{cases} -16r^2 + 3.92 & \text{for } r > 0.7 \\ -5.8408 + 3.92r^2 & \text{for } r \le 0.7. \end{cases},$$

TABLE II. Benchmark examples and corresponding section numbers.

Section	Short name	Problem data	Feature
A	Square domain	$f \neq u_D \neq 0, \chi \equiv 0$	Smooth solution
B	L-shaped domain	$f \neq 0, \chi \equiv u_D \equiv 0$	Corner singularity
C	Square domain	$f \neq \chi \neq u_D \neq 0$	Cusp obstacle
D	Square domain	$f \equiv 1, \chi = \mathrm{dist}(x, \partial\Omega), u_D \equiv 0$	1d contact zone
E	Square domain	$f = -\Delta\chi, \chi = (1-x^2)(y^2-1)$	Nonaffine obstacle

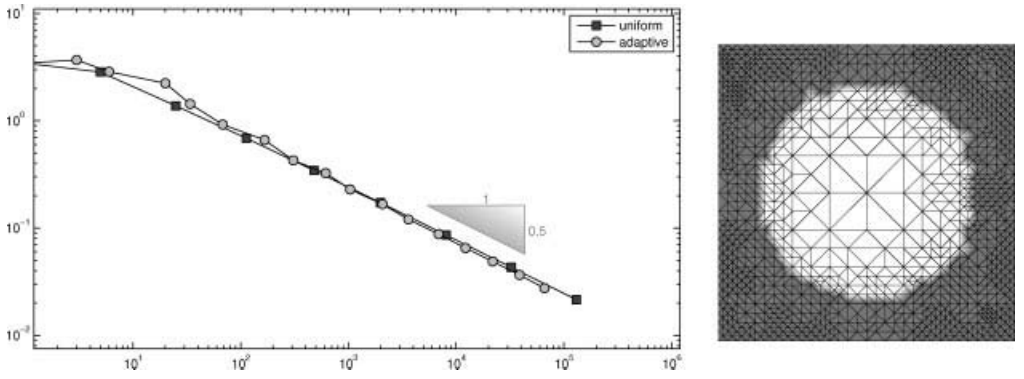

FIG. 2. Convergence history of the energy error as a function of the number of unknowns for uniform and adaptive mesh refinements (left) and adaptive mesh on level $\ell = 9$ (right) in subsection A of section VI.

The exact solution of (1.1) reads

$$u(r,\varphi) = \max\{0, r^2 - 0.49\}^2.$$

The adaptive algorithm of subsection B of section V ran on uniform and adaptive meshes, one is displayed in Fig. 2 on the right-hand side. The contact zone $\{r < 0.7\}$ is less refined while its boundary $\{r = 1\}$ is much more refined than the remaining part of the domain caused by contributions of the extra terms μ_h and $\mathrm{osc}(\Lambda_h, \mathcal{N})$. Since there is no contact along the boundary $\partial\Omega$, the critical boundary term of Remark 4.5 does not arise and there holds efficiency as discussed in part one of this paper.

Figure 2 displays the convergence history of the exact error for uniform and adaptive mesh refinement. Since the solution is smooth, we observe the optimal empirical convergence rate $1/2$ for uniform mesh refinement and marginal improvement by adaptive mesh refinement. The concentration on the boundary of the contact zone indeed improves the convergence rate slightly and supports the heuristic argument of Remark 4.4. In a neighbourhood of the boundary between the contact zone $\{u = \chi\}$ and the noncontact zone $\{u > \chi\}$ the mesh is quasi-uniformly contributed with a relatively small local maximal mesh-size $h_{\max}$.

Figure 3 compares the efficiency indices $I_{\mathrm{xyz}} := \mathrm{GUB}(\eta_{\mathrm{xzy}})/|||e|||$ of the global upper bounds $\mathrm{GUB}(\eta_{\mathrm{xzy}})$ for the six choices of η_{xyz} and the relative contribution $\eta_{\mathrm{xyz}}/\mathrm{GUB}(\eta_{\mathrm{xzy}})$. The efficiency index is around 10 but decreases slowly to values between 1 and 2 except for η_{R} that remains at 10. This is due to the decrease of the extra terms and consistent with the observation that the relative contribution of η_{xyz} becomes more and more dominant. As a consequence, there is a significant impact of the accuracy of η_{xyz} on the efficiency of the global upper bound $\mathrm{GUB}(\eta_{\mathrm{xzy}})$.

B. Benchmark Example 2

The second benchmark example from [3] mimics a typical corner singularity on the L-shaped domain $\Omega = (-2,2)^2 \backslash ([0,2] \times [-2,0])$ with constant obstacle $\chi = \mathcal{I}\chi \equiv 0$ and homogeneous Dirichlet data $u_D \equiv 0$ along $\partial\Omega$, with the right-hand side

$$f(r,\varphi) := -r^{2/3}\sin(2\varphi/3)(7/3\ (\partial g/\partial r)(r)/r + (\partial^2 g/\partial r^2)(r)) - H(r - 5/4),$$
$$g(r) := \max\{0, \min\{1, -6s^5 + 15s^4 - 10s^3 + 1\}\}$$

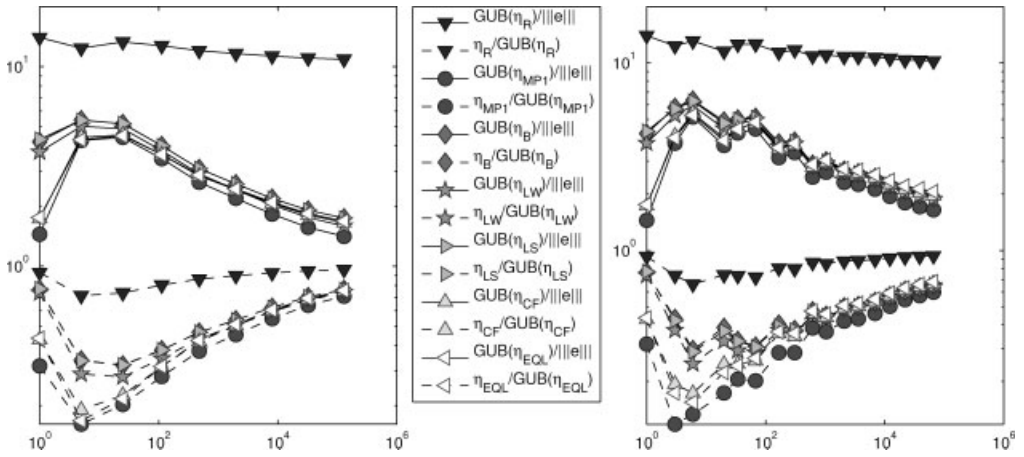

FIG. 3. Efficiency indices of the global upper bound $\mathrm{GUB}(\eta_{\mathrm{xyz}})$ and relative contribution of η_{xyz} to the GUB as functions of the number of unknowns for uniform (left) and adaptive (right) refinement in subsection A of section VI.

for $s := 2(r - 1/4)$ and the Heaviside function H. The exact solution reads

$$u(r, \varphi) := r^{2/3} g(r) \sin(2\varphi/3).$$

The contact zone $\{r > 3/4\}$ has a nonvoid intersection with the boundary $\partial\Omega$. Hence, the critical boundary term of Remark 4.5 does not arise and there holds efficiency as discussed in part one of this paper. Due to the homogeneous Dirichlet data, $w_D \equiv 0$.

The experimental convergence rate for uniform refinement is about 0.4 and adaptive refinement improves it to the optimal value 0.5 and, moreover, it shortens the preasymptotic range depicted in Fig. 4.

Figure 5 monitors the efficiency of the upper bound for uniform and adaptive mesh refinement. In this example, the impact of the extra terms decreases faster and a proper choice of η_{xyz} becomes even more important than in the first two Examples. As known from η_{MP1} in a posteriori error

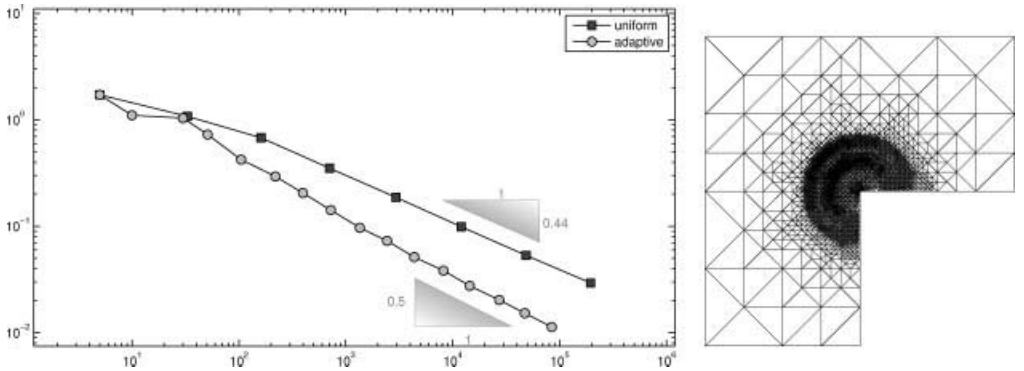

FIG. 4. Convergence history of the energy error as a function of the number of unknowns for uniform and adaptive mesh refinements (left) and adaptive mesh on level $\ell = 9$ (right) in subsection B of section VI.

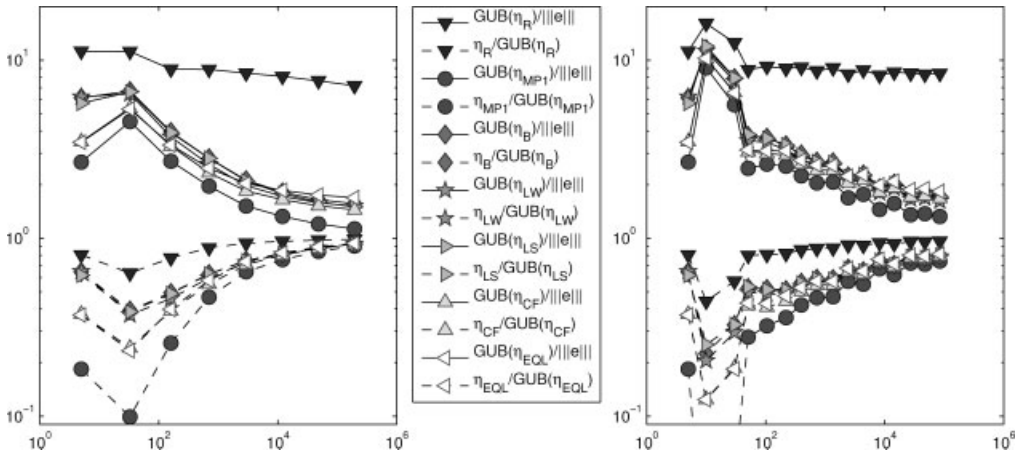

FIG. 5. Efficiency indices of the global upper bound $\mathrm{GUB}(\eta_{\mathrm{xyz}})$ and relative contribution of η_{xyz} to the GUB as functions of the number of unknowns for uniform (left) and adaptive (right) refinement in subsection B of section VI.

estimation for Poisson Problems, the upper bound $\mathrm{GUB}(\eta_{\mathrm{MP1}})$ almost arrives at effiency index 1. Figure 4 visualises that the adaptive mesh refinement spares the contact zone. As in the other Examples, all error estimators except η_{R} perform very well with efficiency indices below 2.

C. Benchmark Example 3

The third example from [5] involves Ω, f and u_D from subsection A of section VI and the obstacle

$$\chi := \max\{-2, 1 - 50\max\{|x|, |y|\}\}$$

with a cusp. Since the exact solution is unknown, the solution on the triangulation $\mathrm{red}^2(\mathcal{T}_\ell)$, which is obtained by two additional red-refinements of $\mathcal{T}_\ell$, acts as an approximation of u for the computation of the energy error $|||u - u_h|||$ on $\mathcal{T}_\ell$. The obstacle is piecewise affine but not on the initial coarse triangulation depicted in Fig. 6 for $\ell = 0$ (left). However, $\chi \leq \mathcal{I}\chi$ leads to a conforming discretization. Therefore, GUB is a valid upper bound.

Figure 6 on the convergence history indicates that the adaptive mesh refinement algorithm recovers the optimal empirical convergence rate. However, Fig. 6 conveys that the efficiency indices of all global upper bounds $\mathrm{GUB}(\eta_{\mathrm{xyz}})$ are above 10 for uniform mesh refinement, and between 6 and 10 for adaptive mesh refinement. The peak at around 300 unknowns in the right-hand side of Fig. 7 is due to a sudden growth of $\mathrm{osc}(\Lambda_h, \mathcal{N})$ possibly caused by the gradual revelation of the real obstacle χ by the adaptive mesh refinement. In this example, the overhead terms μ_h and $\mathrm{osc}(\Lambda_h, \mathcal{N})$ are not of higher order, so there is a strong indication that the heuristic argument of Remark 4.4 fails for nonsmooth obstacles as in this example.

D. Benchmark Example 4

In order to explore the limitations of the theoretical results, the fourth benchmark uses the constant right-hand side $f \equiv 1$ and the nonaffine obstacle $\chi(x, y) = \mathrm{dist}((x, y), \partial\Omega)$ from [3] of the square domain $\Omega = (-1, 1)^2$ with homogeneous Dirichlet data $u_D \equiv w_D \equiv 0$ on $\Gamma_D := \partial\Omega$. The initial

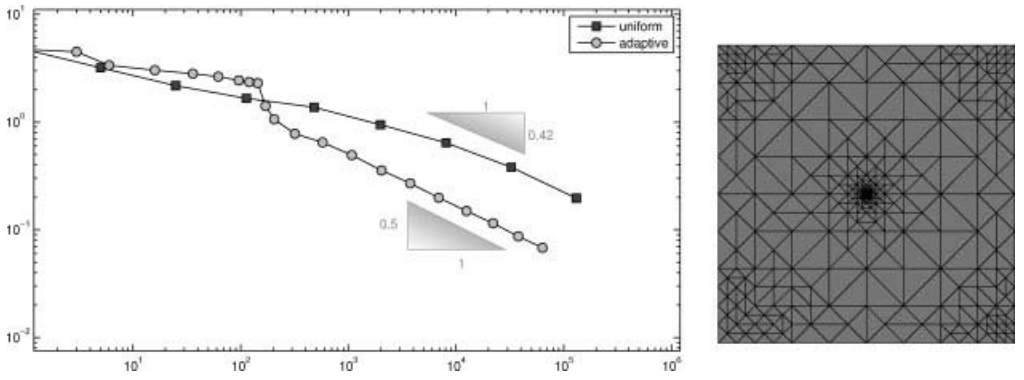

FIG. 6. Convergence history of the energy error as a function of the number of unknowns for uniform and adaptive mesh-refinements (left) and adaptive mesh on level $\ell = 12$ (right) in subsection C of section VI.

triangulation consists of 4 elements such that $\chi = \mathcal{I}\chi$. Since the exact solution is unknown, the solution on the triangulation $\mathrm{red}^2(\mathcal{T}_\ell)$, which is obtained by two additional red-refinements of $\mathcal{T}_\ell$, acts as an approximation of u for the computation of the energy error $|||u - u_h|||$ on $\mathcal{T}_\ell$.

In contrast to the first two benchmarks, the obstacle is not globally affine and the contact zone reduces to the lines

$$\{(x, y) \in (0, 1)^2 | y = x \text{ or } y = 1 - x\}.$$

While uniform refinement yields the optimal empirical convergence rate, the adaptive process has a rather long stagnating preasymptotic range as shown in Fig. 8! But, since the exact energy error is unknown and was approximated by some hierarchic estimator, we cannot say that this holds also for the real energy error. However, the right-hand side of Fig. 8 shows an overkill refinement of the adaptive mesh refinement algorithm along the contact edges due to very high

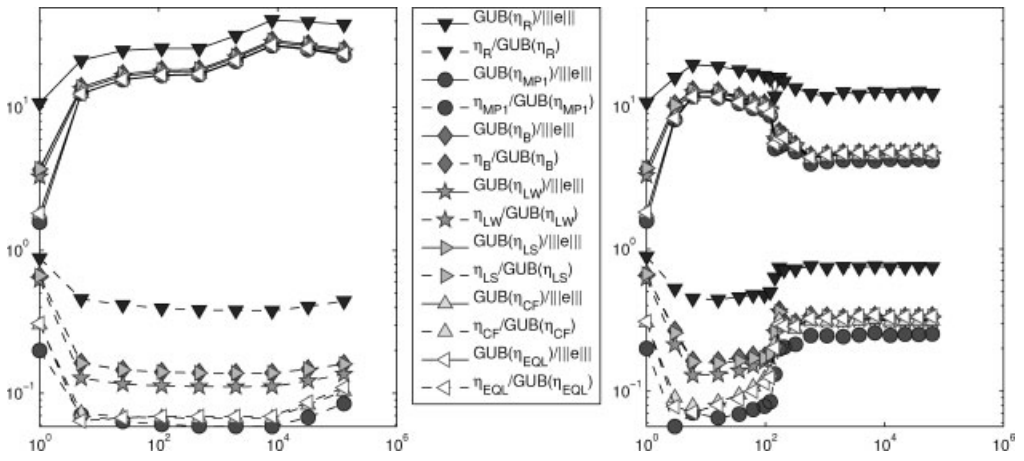

FIG. 7. Efficiency indices of the global upper bound $\mathrm{GUB}(\eta_{\mathrm{xyz}})$ and relative contribution of η_{xyz} to the GUB as functions of the number of unknowns for uniform (left) and adaptive (right) refinement in subsection C of section VI.

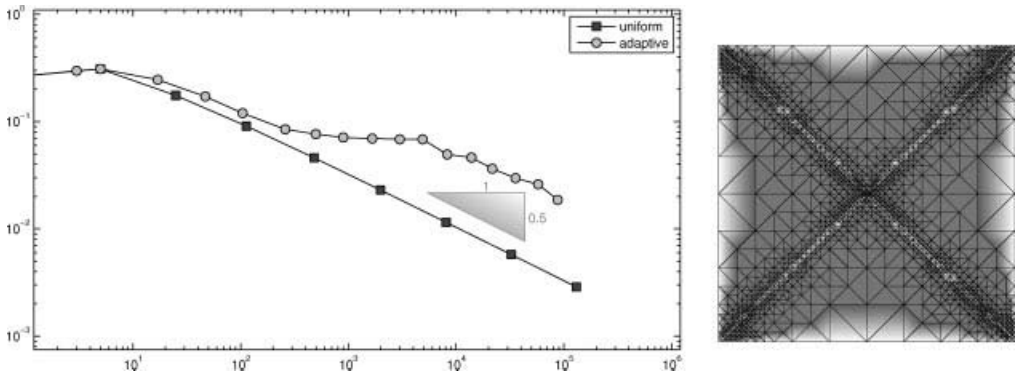

FIG. 8. Convergence history of the energy error as a function of the number of unknowns for uniform and adaptive mesh refinements (left) and adaptive mesh on level $\ell = 9$ (right) in subsection D of section VI.

contributions of the extra terms and nonvanishing edge jumps of ∇u on these edges. A similar behavior was observed in [3] and is expected for every error estimator that is based on edge jumps of ∇u_h.

As the error estimators have been derived for affine obstacles, the efficiency result of Section IV cannot be expected to hold. In fact, Fig. 9 indicates that the upper bound $\mathrm{GUB}(\eta_{\mathrm{xyz}})$ is not efficient with respect to $|||e|||$. The efficiency indices blow up (over 100) for uniform mesh refinement. As the relative contribution of η_{xyz} to the upper bound is nearly constant, the extra terms do not converge faster than η_{xyz}, hence are not of higher order in this example. Adaptive mesh refinement seems to restore the efficiency with efficiency indices around 20, but this is still not rewarding regarding the poor results on the actual error reduction on the produced meshes.

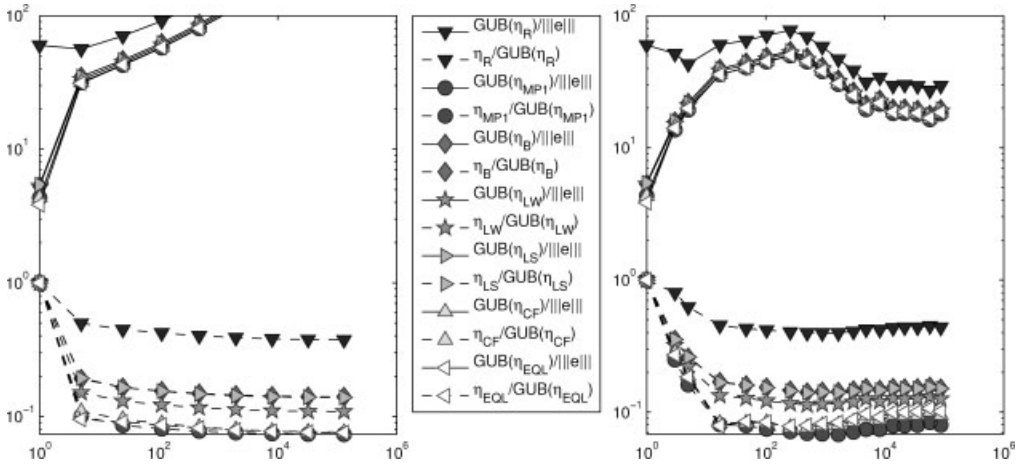

FIG. 9. Efficiency indices of the global upper bound $\mathrm{GUB}(\eta_{\mathrm{xyz}})$ and relative contribution of η_{xyz} to the GUB as functions of the number of unknowns for uniform (left) and adaptive (right) refinement in subsection D of section VI.

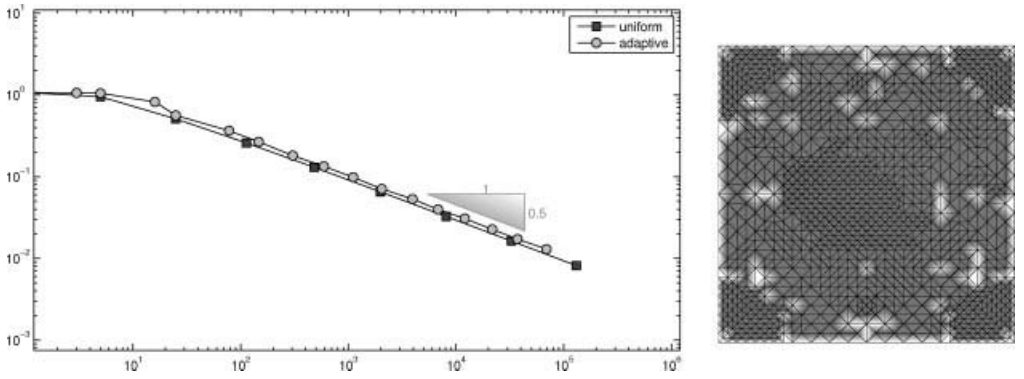

FIG. 10. Convergence history of the energy error as a function of the number of unknowns for uniform and adaptive mesh refinements (left) and adaptive mesh on level $\ell = 9$ (right) in subsection E of section VI.

E. Benchmark Example 5

The last benchmark illustrates that the global upper bound GUB is also applicable to problems with smooth obstacle $\chi(x, y) = -(x^2 - 1)(y^2 - 1)$ for the square domain $\Omega = (-1, 1)^2$ and $f \equiv -\Delta\chi$ from [38] with the exact solution $u \equiv \chi$.

Due to the homogeneous Dirichlet boundary conditions, w_D could be set to 0. But this is a nonconforming obstacle problem with possibly $u_h \notin K$. Hence the proof of property (3.4) would fail. Instead, the choice $w_D := -\min\{0, u_h - \chi\} \geq 0$ after [39] in Theorem 3.2 leads to an admissable test function $u_h + w_D \in K$ and the same global upper bound GUB with the extra terms (only for this section)

$$\mu_h := \left(\int_\Omega (\chi - u_h - w_D) J \Lambda_h \, dx \right)^{1/2} \quad \text{and} \quad |||w_D||| := |||\min\{0, u_h - \chi\}|||.$$

Figure 10 shows that the adaptive mesh refinement barely worsens the empirical convergence rate. Figure 11 displays that efficiency indices are not as good as in the affine examples due to the contribution $|||w_D|||$ that is not of higher order when compared to $|||u - u_h|||$. But we observe a significant improvement of the efficiency indices through adaptive mesh-refinement which reduces the relative contribution $|||w_D|||$ to the GUB.

VII. CONCLUDING REMARKS AND COMMENTS

A. Error Control via Error Estimators for Poisson problems

A posteriori error estimators η_{xyz} for Poisson problems can easily be applied by modification of the right-hand side after Braess [6] and lead to reliable error estimators for obstacle problems with efficiency indices in the range of 1–3. This enables guaranteed error control for variational inequalities with efficiency almost as accurate as for the variational equations–at least for affine obstacles. The global upper bound GUB(η_{xyz}) consists of other contributions that may dominate on triangulations where the boundary of the contact zone is only roughly resolved. Therefore, we included their local contributions in the refinement indicators, cf. $\eta(T)$ in Subsection B of section V. Undisplayed experiments have convinced us that without those extra terms from $\mu_h + \text{osc}(\Lambda_h, \mathcal{N}) + |||w_D|||$, the adaptive mesh refinement yields inferior efficiency of the GUB.

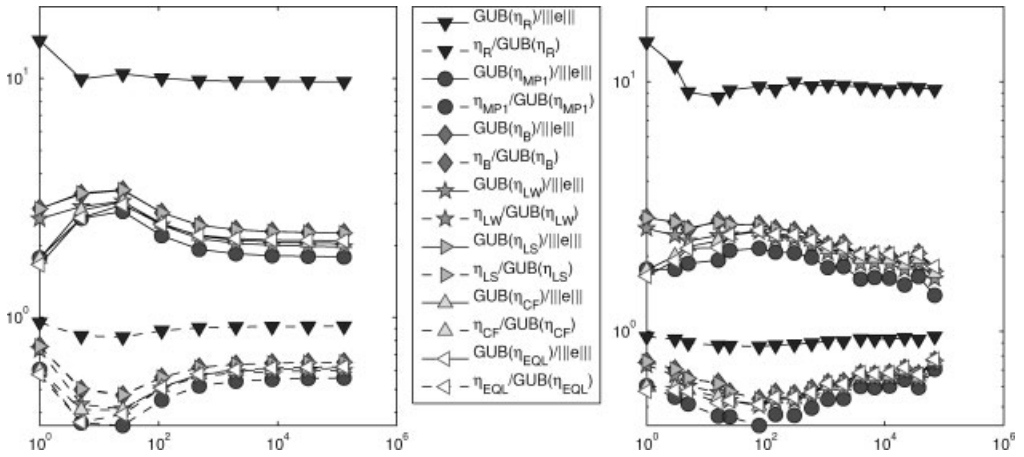

FIG. 11. Efficiency indices of the global upper bound $\mathrm{GUB}(\eta_{\mathrm{xyz}})$ and relative contribution of η_{xyz} to the GUB as functions of the number of unknowns for uniform (left) and adaptive (right) refinement in subsection E of section VI.

B. Efficiency

For affine obstacles as in subsections A and B of section VI, we observe efficiency of $\mathrm{GUB}(\eta_{\mathrm{xyz}})$ and reasonable adaptive mesh refinement. As a limitation of the theoretical predictions, subsection D of section VI illustrates that efficiency cannot be guaranteed for nonaffine obstacles. In that example, none of the a posteriori error estimators leads to an efficient GUB and the error reduction through adaptive mesh refinement is even inferior to uniform mesh-refinement. This is also observed for the error estimator suggested in [3]. As shown in [7], the edge contributions appear to be responsible for the loss of efficiency. Hence, all estimators that are based on edge contributions are expected to fail in this example; compare also [8].

C. Accurate Error Control Pays Off

The solve of an obstacle problem is more costly than the solve of a Poisson problem. Therefore, a sharp error estimator that prevents unnecessary over-refinements is even more important for a termination criterion. As for Poisson problems, apart from the residual-based error estimator η_{R}, all tested error estimators η_{xyz} are highly accurate, at least in subsection A, B, and E of section VI where the overhead terms μ_h and $\mathrm{osc}(\Lambda_h, \mathcal{N})$ become small. Among the tested error estimators, all more elaborated error estimators performed almost equally well. However, η_{EQL} and η_{CF} solve the local problems only approximately, so they are only lower bounds for their associated guaranteed upper bounds. This may lead to a preference of the least-square error estimator η_{LS} or the equilibration error estimators η_{B} of Braess or η_{LW} of Luce-Wohlmuth.

D. Adaptive Mesh Refinement

The adaptive mesh design of this article is based on the explicit residual-based error estimator η_{R}. Undisplayed numerical experiments without mesh-refinement indication based on η_{xyz} from Table I lead to comparable results. This was also observed for adaptive mesh refinement algorithms for Poisson problems in [23, 24].

References

1. C. Carstensen, J. Hu, and C. Loebhard, Optimality of a conforming adaptive finite element method for an affine obstacle problem, in preparation.
2. D. Braess, C. Carstensen, and R. H. W. Hoppe, Convergence analysis of a conforming adaptive finite element method for an obstacle problem, Numer Math 107 (2007), 455–471.
3. S. Bartels and C. Carstensen, Averaging techniques yield reliable a posteriori finite element error control for obstacle problems, Numer Math 99 (2004), 225–249.
4. R. H. Nochetto, K. G. Siebert, and A. Veeser, Fully localized a posteriori error estimators and barrier sets for contact problems, SIAM J Numer Anal 42 (2005), 2118–2135 (electronic).
5. R. H. Nochetto, K. G. Siebert, and A. Veeser, Pointwise a posteriori error control for elliptic obstacle problems, Numer Math 95 (2003), 163–195.
6. D. Braess, A posteriori error estimators for obstacle problems—another look, Numer Math 101 (2005), 415–421.
7. D. Braess, R. H. W. Hoppe, and J. Schöberl, A posteriori estimators for obstacle problems by the hypercircle method, Comput Vis Sci 11 (2008), 351–362.
8. A. Veeser, Efficient and reliable a posteriori error estimators for elliptic obstacle problems, SIAM J Numer Anal 39 (2001), 146–167 (electronic).
9. D. Kinderlehrer and G. Stampacchia, An introduction to variational inequalities and their applications, Pure and applied mathematics, Vol. 88, Academic Press Inc. [Harcourt Brace Jovanovich Publishers], New York, 1980.
10. E. Zeidler, Nonlinear functional analysis and its applications, Springer-Verlag, New York, 1986-1997.
11. J.-F. Rodrigues, Obstacle problems in mathematical physics, North-Holland mathematics studies, Vol. 134, North-Holland Publishing Co., Amsterdam, 1987; Notas de Matemática [Mathematical Notes], 114.
12. S. C. Brenner and L. R. Scott, The mathematical theory of finite element methods, Texts in applied mathematics, Vol. 15, Springer-Verlag, New York, 1994.
13. P. G. Ciarlet, The finite element method for elliptic problems, Studies in mathematics and its applications, Vol. 4, North-Holland Publishing Co., Amsterdam, 1978.
14. M. Ainsworth and J. T. Oden, A posteriori error estimation in finite element analysis, Wiley, New York, 2000.
15. R. Becker and R. Rannacher, A feed-back approach to error control in finite element methods: basic analysis and examples, Numer Math 4 (1996), 237–264.
16. I. Babuška and T. Strouboulis, The finite element method and its reliability, Oxford University Press, New York, 2001.
17. K. Eriksson, D. Estep, P. Hansbo, and C. Johnson, Computational differential equations, Cambridge University Press, Cambridge, 1996.
18. R. Verfürth, A review of a posteriori error estimation and adaptive mesh refinement techniques, Wiley-Teubner, 1996.
19. S. Repin, A Posteriori estimates for partial differential equations, Radon series on computational and applied mathematics, Vol. 4, Walter de Gruyter, Berlin, 2008.
20. S. Repin, S. Sauter, and A. Smolianski, A posteriori error estimation for the dirichlet problem with account of the error in the approximation of boundary conditions, Computing 70 (2003), 205–233.
21. R. Luce and B. I. Wohlmuth, A local a posteriori error estimator based on equilibrated fluxes, SIAM J Numer Anal 42 (2004), 1394–1414.
22. D. Braess, Finite elements-theory, fast solvers, and applications in solid mechanics, Cambridge University Press, New York, 2007.

23. S. Bartels, C. Carstensen, and R. Klose, An experimental survey of a posteriori Courant finite element error control for the Poisson equation, Adv Comput Math 15 (2002), 79–106, 2001. A posteriori error estimation and adaptive computational methods.

24. C. Carstensen and C. Merdon, Estimator competition for Poisson problems, J Comp Math 28 (2010), 309–330 (electronic).

25. C. Carstensen, Quasi-interpolation and a posteriori error analysis in finite element methods, M2AN Math Model Numer Anal 33 (1999), 1187–1202.

26. C. Carstensen and R. Verfürth, Edge residuals dominate a posteriori error estimates for low order finite element methods, SIAM J Numer Anal 36 (1999), 1571–1587 (electronic).

27. S. Bartels, C. Carstensen, and G. Dolzmann, Inhomogeneous Dirichlet conditions in a priori and a posteriori finite element error analysis, Numer Math 99 (2004), 1–24.

28. S. C. Brenner and C. Carstensen, Finite element methods, Chapter 4, In E. Stein, R. de Borst, and T. J. R. Hughes, editors, Encyclopedia of Computational Mechanics, John Wiley and Sons, 2004.

29. C. Carstensen, A unifying theory of a posteriori finite element error control, Numer Math 100 (2005), 617–637.

30. C. Carstensen, M. Eigel, R. H. W. Hoppe, and C. Loebhard, Review of unified a posteriori finite element error control, in preparation.

31. C. Carstensen and C. Merdon, Computational survey on a posteriori error estimators for nonconforming finite element methods for the poisson problem, Submitted for publication.

32. R. H. Nochetto and L. B. Wahlbin, Positivity preserving finite element approximation, Math Comp 71 (2002), 1405–1419 (electronic).

33. C. Carstensen and S. Bartels, Each averaging technique yields reliable a posteriori error control in fem on unstructured grids part I: Low order conforming, nonconforming, and mixed fem, Math Comp 71 (2002), 945–969.

34. C. Carstensen and S. A. Funken, Fully reliable localised error control in the fem, SIAM J Sci Comput 21 (1999), 1465–1484 (electronic).

35. C. Carstensen, All first-order averaging techniques for a posteriori finite element error control on unstructured grids are effective and reliable, Math Comp 73 (2004), 1153–1165.

36. D. Braess and J. Schöberl, Equilibrated residual error estimator for edge elements, Math Comp 77 (2008), 651–672.

37. P. Ladeveze and D. Leguillon, Error estimate procedure in the finite element method and applications, SIAM J Numer Anal 20 (1983), 485–509.

38. C. Gräser and R. Kornhuber, Multigrid methods for obstacle problems, J Comput Math 27 (2009), 1–44.

39. R. S. Falk, Error estimates for the approximation of a class of variational inequalities, Math Comput 28 (1974), 963–971.

40. A. Veeser, On a posteriori error estimation for constant obstacle problems, Numerical methods for viscosity solutions and applications (Heraklion, 1999), Ser. Adv. Math. Appl. Sci., Vol. 59, World Sci. Publ., River Edge, NJ, 2001, pp. 221–234.